

Photonic-Wire Laser

J. P. Zhang, D. Y. Chu, S. L. Wu, and S. T. Ho

*Department of Electrical Engineering and Computer Science, The Technological Institute, Northwestern University,
2145 Sheridan Road, Evanston, Illinois 60208*

W. G. Bi and C. W. Tu

Department of Electrical and Computer Engineering, University of California at San Diego, La Jolla, California 92093-0407

R. C. Tiberio

National Nanofabrication Facility, Cornell University, Ithaca, New York 14853-5403

(Received 25 May 1995)

We have achieved lasing in a strongly guided semiconductor waveguide with mode area as small as $0.02 \mu\text{m}^2$ ($\lambda = 1.4 \mu\text{m}$). The lasing action takes advantage of the large enhancement of stimulated emission in the waveguide and its suppression of unwanted dipole emission. We call the waveguide a photonic wire. The laser cavity is a high- Q microcavity ring resonator formed by the photonic wire and has a small cavity mode volume of $0.27 \mu\text{m}^3$. The lasing behaviors are consistent with theory. Laser outputs can be obtained via photon tunneling to adjacent waveguides. The laser realized will allow us to study spontaneous emission and lasing in nanofabricated waveguide structures.

PACS numbers: 42.60.Da, 42.50.Lc

An interesting problem in quantum optics is the modification of spontaneous emission in artificial photonic structures such as microcavities, photonic band-gap structures, microdroplets, and low-dimensional photonic structures [1–5]. For example, one can use these structures to control spontaneous emission as well as stimulated emission into a particular electromagnetic field mode. Such control enables one to realize novel lasers with dimensions and properties much different from lasers with conventional structures. The laser properties that could be manipulated include the lasing thresholds, the population inversion, the laser modulation rates, and the carrier dynamics such as their decay rates and response times. Some of these properties may have novel photonic and electronic applications in the future.

We report the realization of lasers based on low-dimensional photonic structures called photonic-wire structures. Photonic-wire structures are strongly guided one-dimensional waveguides with tightly confined mode area. Specifically, we may call a strongly guided waveguide a photonic wire if a large percentage of spontaneous emission can be channeled into the lowest-order guided mode. An example is sketched in Fig. 1, where a strongly guided waveguide is made up of a high-refractive-index semiconductor core ($n = 3.4$) surrounded by low-refractive-index cladding such as air ($n = 1$) or SiO_2 ($n = 1.5$). The cavities of the lasers realized are high- Q microcavity ring resonators formed by the strongly guided waveguides.

The fraction of spontaneous emission channeled into the lasing mode is called the spontaneous-emission coupling efficiency β and is an important factor that determines the lasing threshold. A large β value can increase the effective gain of the cavity, making it possible to

achieve lasing in a small cavity and to attain low lasing threshold [1,6]. We will discuss how the laser waveguide parameters affect spontaneous emission and how they can be chosen to achieve very large β value. We then discuss our experiment on the realization of photonic-wire microcavity semiconductor lasers and relate our initial experimental observation to theory.

Recently, we have studied theoretically the modification of spontaneous emission in a strongly guided cylindrical dielectric waveguide as shown in Fig. 2(a), where d is the waveguide diameter [3]. In the study, the total spontaneous emission rate γ_{tot} was decomposed into

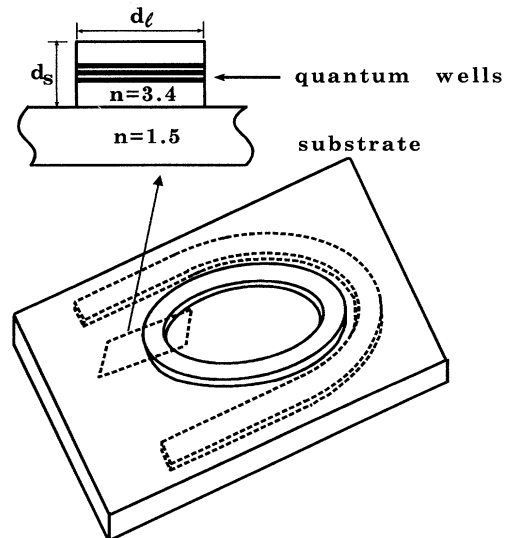


FIG. 1. Schematic diagram of the photonic-wire ring lasers. The high-refractive-index guided core is surrounded by low-refractive-index claddings such as air and SiO_2 .

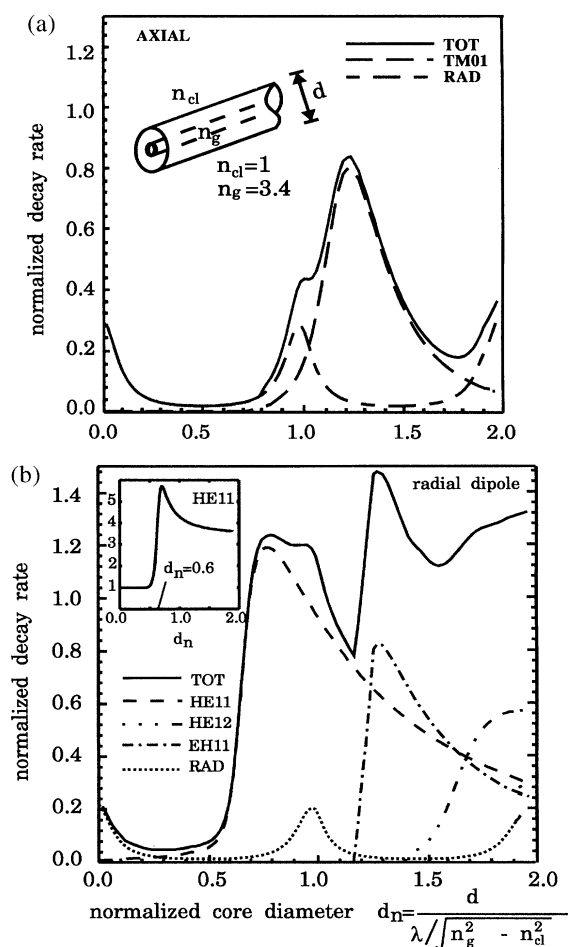


FIG. 2. Normalized decay rates. (a) The normalized decay rates $\gamma_g(\text{TM}_{01})$, γ_R , and the total normalized decay rate γ_{tot} of the axial dipole versus the normalized core diameter d_n . (b) The normalized decay rates $\gamma_g(\text{HE}_{11})$, $\gamma_g(\text{HE}_{12})$, $\gamma_g(\text{EH}_{11})$, γ_R , and the total normalized decay rate γ_{tot} of the radial dipole versus the normalized core diameter. Inset shows the drop in photon density of states for the HE_{11} mode at $d_n = 0.6$.

two components, namely, the guided mode and radiation mode components, denoted by γ_g and γ_R , respectively, with $\gamma_{\text{tot}} = \gamma_g + \gamma_R$. The radiation modes are modes that escape the waveguides. The value for γ_g was calculated as a sum over the spontaneous emission rate into each waveguide mode denoted by γ_m , where m is the mode index (i.e., $\gamma_g = \sum_m \gamma_m$).

When the active medium is excited, each radiating dipole can be decomposed into three mutually orthogonal dipoles: two along the radial directions (radial dipoles) and one along the waveguide axis (axial dipole). Let the refractive indices of the waveguide core and cladding be n_g and n_{cl} , respectively. Figures 2(a) and 2(b) plot the emission rates as a function of the normalized waveguide diameter $d_n = d/(\lambda/n_{\text{ave}})$ ($n_{\text{ave}} \equiv \sqrt{n_g^2 - n_{cl}^2}$ and λ is free-space wavelength) for the cases of an axial dipole

and a radial dipole, respectively [3]. In the plots the emission rates are normalized by the bulk rate [3]. From Fig. 2(b), we see that if $0.65 < d_n < 0.85$, the radial dipole emission can be channeled predominantly into the lowest-order guided mode (HE_{11}). From Fig. 2(a), we see that the axial dipole emission is suppressed at $d_n < 0.85$. For the case of a rectangular waveguide shown in Fig. 1, further control of emission could be achieved. Let us assume that the active medium is a few quantum wells parallel to d_ℓ and located at the midpoint of d_s (see Fig. 1). The decay rates relevant to this case have been studied by Ho, McCall, and Slusher in the situation where $d_\ell \gg d_s$ [2]. Below, we will use normalized waveguide dimensions defined by $d_{sn} \equiv d_s/(\lambda/n_{\text{ave}})$ and $d_{\ell n} \equiv d_\ell/(\lambda/n_{\text{ave}})$. The results are shown in Fig. 2 of Ref. [2], plotting the total decay rates of the horizontal and vertical dipoles as a function of d_{sn} . The figure suggests that in this geometry emission from dipoles perpendicular to the quantum wells (vertical dipoles) can be partially suppressed compared to emission from dipoles to the quantum well (horizontal dipoles) provided $d_{sn} < 0.5$ and emission from the horizontal dipoles into the lowest-order mode is maximum at $0.2 < d_{sn} < 0.4$. We note that, in addition, the quantum wells by themselves also have strongly preferential horizontal dipole emission [7].

Hence, with appropriate waveguide design it is possible to suppress both the vertical and axial dipole emission so that only the horizontal dipole emission dominates. The estimated waveguide dimensions for which this could be achieved are $0.2 < d_{sn} < 0.4$ (to suppress vertical dipole) and $0.65 < d_{\ell n} < 0.85$ (to suppress axial dipole and enhance horizontal dipole emission into the lowest-order guided mode). The estimation here is sufficient to guide our initial design. A better estimate could be obtained in the future by solving for rectangular waveguide modes. In our experiment, we have $n_g = 3.3$ and $n_{cl} \approx 1$ and the photonic wire fabricated has $d_s \approx 0.4\lambda/n_{\text{ave}} = 0.18 \mu\text{m}$ and $d_\ell \approx 0.85\lambda/n_{\text{ave}} = 0.38 \mu\text{m}$.

The emission rates into the radiation modes in Fig. 2 can be seen to undergo resonances, which is due to the cavity effect formed by the opposite surfaces of the waveguide [3]. From Fig. 2(b), we see that with $d_\ell \approx 0.75\lambda/n_{\text{ave}}$ about 95% of the spontaneous emission can be channeled into the lowest-order guided mode. It reduces to 70% when the cavity resonances are averaged out and the emissions from the vertical and axial dipoles are accounted for [3]. Thus, for a ring cavity with bidirectional lasing in the HE_{11} mode, the β value could be around 0.35 (70% divided by two directions). This is much higher than the usual semiconductor laser cavities, typically with $\beta \approx 10^{-5}$ [1]. It is also higher than microdisk lasers with $\beta \approx 0.1$, which can be achieved only with a disk diameter smaller than $3 \mu\text{m}$ [4].

In our experiment, InGaAsP/InGaAs epitaxial layers grown by molecular beam epitaxy on an InP substrate were used to realize the photonic-wire lasers. The epitaxial layers form a $0.19 \mu\text{m}$ thick InGaAsP/InGaAs laser

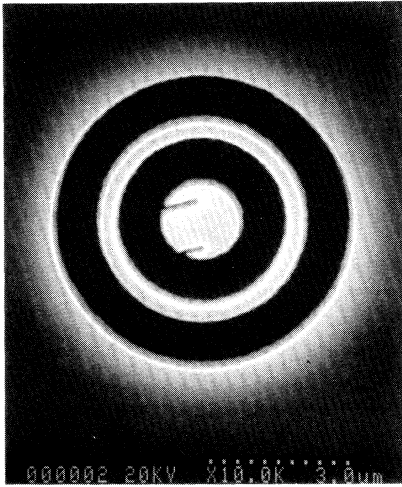


FIG. 3. Scanning electron microscope image of a $4.5 \mu\text{m}$ diameter photonic-wire ring laser with $0.4 \mu\text{m}$ waveguide.

structure. Within the structure, three 100 \AA quantum wells ($\text{In}_{0.53}\text{Ga}_{0.47}\text{As}$) were separated by 100 \AA barriers ($\text{In}_{0.84}\text{Ga}_{0.16}\text{As}_{0.33}\text{P}_{0.67}$). They were sandwiched by two 700 \AA $\text{In}_{0.84}\text{Ga}_{0.16}\text{As}_{0.33}\text{P}_{0.67}$ layers on both sides.

Nanofabrications involving electron-beam (E -beam) lithography and reactive ion etching (RIE) were used to fabricate the lasers. A wafer bonding and backetching technique described below was used to transfer the thin ring on top of a low-refractive-index SiO_2 cladding on GaAs substrate. First, a 800 \AA thick SiO_2 was deposited on the wafer via plasma-enhanced chemical-vapor deposition (PECVD). E -beam lithography was used to write the ring laser pattern on PMMA coated on the SiO_2 layer. The pattern was transferred down to the SiO_2 layer by etching away the unmasked region using RIE with CHF_3 etchant gas under 31 mTorr pressure and 60 W plasma power, and then the PMMA was removed. The pattern on SiO_2 then formed the mask for subsequent etching of the InGaAsP layer. RIE was again used to etch the rings down vertically through the $0.19 \mu\text{m}$ thick InGaAsP/InGaAs epitaxial layers into the InP substrate. In this step, we used a gas mixture of methane, hydrogen, and argon with a ratio of 10:34:10 under 45 mTorr and 90 W plasma power. To place the thin ring laser structure on a low-refractive-index material, the substrate was removed via the following technique. The RIE etched sample and a sample of GaAs substrate were deposited with $0.75 \mu\text{m}$ thick SiO_2 using PECVD. The two samples were then SiO_2 face-to-face bonded together using acrylic. Finally, a highly selective etchant ($\text{HCl}:\text{H}_3\text{PO}_4$, 1:1) was used to remove the InP substrate, leaving the ring laser structure on $1.5 \mu\text{m}$ thick SiO_2 above the GaAs substrate. Figure 3 shows the photonic-wire ring laser fabricated with $4.5 \mu\text{m}$ ring diameter and $0.4 \mu\text{m}$ waveguide width (the waveguide thickness is $0.19 \mu\text{m}$).

The photonic-wire ring lasers were optically pumped with a 514 nm argon-ion laser modulated with 1% duty

cycle in a vacuum-assisted Joule-Thomson refrigerator at 85 K [5]. The beam was focused with a $40\times$ microscope objective lens to a size larger than the size of the lasers. The scattered output light was collected from the top of each laser via the objective lens. The emission spectrum was measured with a method similar to Ref. [5].

In our experiment, photonic-wire ring lasers with $4.5 \mu\text{m}$ diameter and waveguide widths of 0.25 and $0.4 \mu\text{m}$ were fabricated. The typical emission spectra of the photonic-wire laser with a waveguide width of $0.4 \mu\text{m}$ are shown in Fig. 4, indicating lasing at 1403 nm . The dashed curve is the spectrum at around threshold where the peak pump power absorbed by the laser is approximately $95 \mu\text{W}$. The lasing power as a function of the peak pump power is shown in the inset of Fig. 4. Its spectral linewidth at 1.5 threshold was measured to be about 0.5 nm with a spectrum analyzer resolution of 0.1 nm . The cavity Q value was estimated to be $Q = 300$ from the emission linewidth of the enhanced photoluminescence below threshold near the cavity resonance. This corresponds to a waveguide loss of 2% per round trip due to the average corrugation of around $0.02 \mu\text{m}$ on the waveguide side walls.

In order to obtain light output, in some variation we have fabricated a waveguide adjacent to the ring laser as shown by the dotted line in Fig. 1. We have obtained light output from the waveguide, and the result will be published elsewhere.

We found that while the laser with $0.4 \mu\text{m}$ waveguide width lased, those with $0.25 \mu\text{m}$ waveguide width did not. To compare with theory, we see from Fig. 2(b) that when d_n is smaller than 0.65 ($d \approx 0.3 \mu\text{m}$), the emission into the lowest-order guided mode is highly suppressed. In that regime, emission into the radiation mode dominates, and the β value drops drastically. This large drop in emission into the lowest-order mode is due to a large plunge in the photon density of states as shown in the inset of Fig. 2(b) as well as an increase in the mode area at very small waveguide dimensions. As the $0.25 \mu\text{m}$ waveguide has $d_\ell \approx d_s < 0.65$, the laser structure will have a low β value and low gain, and hence cannot lase. While the experimental observation is consistent with theory, we should point out that the increased scattering loss in the $0.25 \mu\text{m}$ waveguide can also be a factor that affects lasing.

In order to understand interesting operational parameters associated with the photonic-wire laser, we can use the following laser rate equations [1]:

$$\frac{dI(t)}{dt} = -\gamma_c I(t) + GI(t) + R_L, \quad (1)$$

$$\frac{dN_u(t)}{dt} = -R - GI(t) + C(t), \quad (2)$$

where $I(t)$ is the number of photons in the lasing mode. $N_u(t)$ and $N_g(t)$ are the number of gain-medium atoms or excitons in the excited state (upper level) and ground state, respectively. The total number of atoms is given by $N_A = N_u(t) + N_g(t)$. In Eq. (1), γ_c is the photon

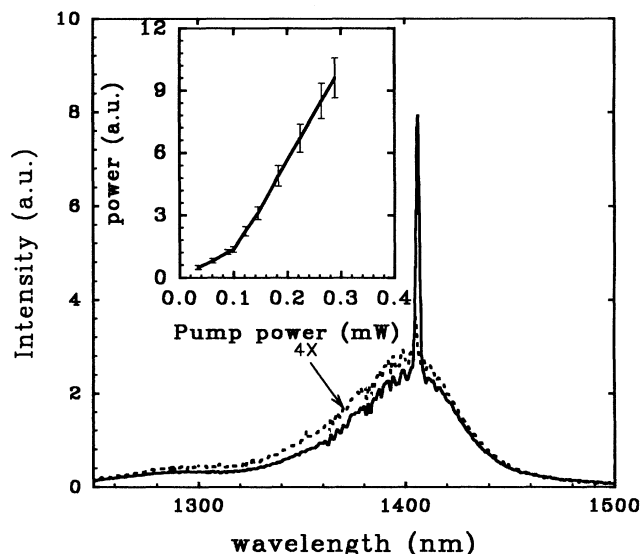


FIG. 4. Spectra of a 4.5 μm photonic-wire ring laser with 0.4 μm waveguide. The solid line and the dashed line were measured above (1.5 threshold) and near threshold, respectively. Inset shows the measured lasing power as a function of peak pump power.

cavity decay rate, G is the gain coefficient given by $G = \gamma_L[N_u - N_g]$, and R_L is the spontaneous emission rate into the lasing mode given by $R_L = \gamma_L N_u$. In Eq. (2), $C(t)$ is the population pumping rate and R is the total spontaneous emission rate with $R = (\gamma_{\text{oth}} + \gamma_L)N_u$, where $\gamma_{\text{oth}}N_u$ is the spontaneous emission rate into all nonlasing modes and $\gamma_{\text{tot}} = \gamma_{\text{oth}} + \gamma_L$ is the total spontaneous decay rate of an excited atom. Note that G is dependent on β and can be written as $G = \gamma_{\text{tot}}\beta[N_u - N_g]$, where $\beta = \gamma_L/\gamma_{\text{tot}}$. By setting the time derivatives to zero, these equations can be used to solve for the steady-state population inversion $N_{u0} - N_{g0}$ and the photon number I_0 as a function of the pumping rate C . One can then estimate the lasing spectral linewidth using $\Delta\nu_L = (Gn_{\text{sp}}/4\pi I_0)(1 + \alpha^2)$ [8].

For the 4.5 μm laser with 0.4 μm waveguide having a top surface area of $A_D \approx 5 \mu\text{m}^2$, we assume a typical transparency carrier number per unit area of $\rho_{\text{tr}} = 1.3 \times 10^{12}/\text{cm}^2$ for a single 100 \AA thick quantum well giving $N_A = 3 \times 2\rho_{\text{tr}}A_D \approx 400\,000$ for three wells. We take $\gamma_{\text{tot}} = 0.3 \times 10^9 \text{ sec}^{-1}$, $\alpha = 3$, and $\gamma_c = 2 \times 10^{11} \text{ sec}^{-1}$ (for $Q = 300$) [8]. We obtain a theoretical laser linewidth of about 0.7 nm for the case of Fig. 4 at 1.5 threshold, which is close to experimental observation. It can be shown that $\Delta\nu_L$ scales as $\Delta\nu_L \propto \sqrt{\beta}\gamma_c$, which indicates that the large observed linewidth is consistent with the large theoretical β value. A more detailed comparison between theory and experiment will be a subject of future studies.

In summary, we have demonstrated the photonic-wire lasers. The laser is formed by a strongly guided single-mode waveguide with a mode area of 0.02 μm^2 and phys-

ical dimensions of 0.19 $\mu\text{m} \times 0.4 \mu\text{m}$. The small mode area gives a large spontaneous-emission coupling efficiency of around 35%. Theory shows that with proper choice of waveguide dimensions, the dipole emission can be highly nonisotropic enabling the dominance of emission from a single dipole orientation. We found theoretically that photonic-wire lasers must have a minimum waveguide cross-sectional area, below which the β value can become small and lasing will cease. This is consistent with our experimental observation. The observed lasing linewidth of 0.5 nm is also consistent with theory. The laser demonstrated has a mode volume of only 0.27 μm^3 and a material volume of 1 μm^3 , which is around the smallest laser ever realized. Our experimental realization will allow new possibilities to explore the physics of spontaneous emission, lasing, and carrier dynamics in nanofabricated waveguides and microcavities.

Work at Northwestern University was supported by Advanced Research Project Agency Contract No. F30602-94-1-0003 and NSF Faculty Early Career Development Award No. ECS-9502475. Work at UCSD was supported by NSF Grant No. DMR-9202692. This work was performed in part at the National Nanofabrication Facility supported by NSF Grant No. ECS-8619049 and the Northwestern University Material Research Center supported by NSF Grant No. DMR-9120521.

- [1] Y. Yamamoto, *Coherence, Amplification, and Quantum Effects in Semiconductor Laser* (John Wiley & Sons, New York, 1991), and references therein; E. Yablonovitch and T.J. Gmitter, Phys. Rev. Lett. **63**, 1950 (1989); S.D. Brorson, H. Yokoyama, and E.P. Ippen, IEEE J. Quantum Electron. **26**, 1492 (1990); J.R. Snow, S.-X. Qian, and R.K. Chang, Opt. Lett. **10**, 37 (1985); A.J. Campillo, J.D. Eversole, and H.-B. Lin, Phys. Rev. Lett. **67**, 437 (1991).
- [2] S.T. Ho, S.L. McCall, and R.E. Slusher, Opt. Lett. **18**, 909 (1993).
- [3] D.Y. Chu and S.T. Ho, J. Opt. Soc. Am. B **10**, 381 (1993).
- [4] R.E. Slusher, A.F.J. Levi, U. Mohideen, S.L. McCall, S.J. Pearton, and R.A. Logan, Appl. Phys. Lett. **63**, 1310 (1993); M.K. Chin, D.Y. Chu, and S.T. Ho, J. Appl. Phys. **75**, 3302 (1993).
- [5] D.Y. Chu, M.K. Chin, W.G. Bi, H.Q. Hou, C.W. Tu, and S.T. Ho, Appl. Phys. Lett. **65**, 3167 (1994).
- [6] According to quantum mechanics, the spontaneous emission rate in any field mode is equal to its stimulated emission rate with one photon. An increase in the spontaneous-emission coupling efficiency can lead to an increase in stimulated emission and hence gain, which reduces lasing threshold. See also comments on gain G after Eq. (2).
- [7] M. Yamanishi and I. Suemune, Jpn. J. Appl. Phys. **23**, L35 (1984).
- [8] G. Bjork, A. Karlsson, and Y. Yamamoto, Appl. Phys. Lett. **60**, 304 (1992); C.H. Henry, IEEE J. Quantum Electron. **QE-19**, 1391 (1983).

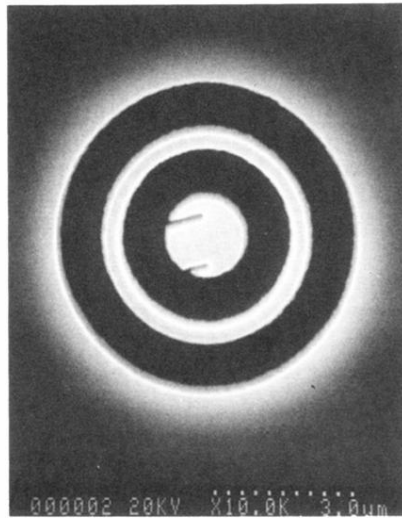


FIG. 3. Scanning electron microscope image of a $4.5 \mu\text{m}$ diameter photonic-wire ring laser with $0.4 \mu\text{m}$ waveguide.